

Air Flow Management Inside Data Center

Abubaker Mohamed Elamin Ali Gabir¹, Hassan A/Latif Osman² and Ali Mohamed Ali Alseory³

¹Ph.D. Candidate, School of Mechanical Engineering,
Sudan University of Science & Technology, Khartoum, Sudan
abubakermohamed@live.com

²Associate Professor, Mechanical Department,
Sudan University of Science & Technology, Khartoum, Sudan
hassan3628@gmail.com

³Associate Professor, Mechanical Department,
Khartoum University, Khartoum, Sudan
aseory10@gmail.com

Abstract

This paper deals with air flow management inside open aisle data center. First, the data center components are introduced and cooling challenges are described. Data center with raised floor is investigated for different ways of air flow management and control. Icepack (Computational Fluid Dynamics, CFD) is used to simulate data center. The influence of gaps between racks has been showed & corrected then the data center was explored based on rack level using beta index and energy utilization index. The effect of air flow outlet angle, supply air temperature, tile open area and end effect are highlighted. Finally, optimal operating parameters for data center are determined.

Keywords: Data Center, Computational fluid dynamics, Icepack, Raised floor, β index, Utilization energy Index.

1. Introduction

Data center is a facility hosting servers, processors, computer equipment's and auxiliary systems. These systems are power supply, air conditioning, and environment monitoring, firefighting and security systems.

Telecom equipment's are installed inside racks. The racks are installed on a tile floor that is raised above the real solid floor. These racks are organized front to front and back to back to form aisles. Cold aisle is where the cold air is supplied & hot aisle is where the exhaust air is discharged from racks.

The raised-floor arrangement is very flexible because it is easy to change the layout of racks

by rearranging the perforated tiles. The floor tiles are removable and some of the solid tiles can be replaced by grilles or perforated tiles. Computer room air conditioner unit (CRAC) pump cold air into the space below the raised floor.

Cooling system must be designed to maintain operating condition within recommended range using minimum power consumption. There are three main ways for the energy saving inside data centers: (1) selection of air conditioner with high energy efficiency ratio; (2) managing of auxiliary systems; and (3) optimization of air flow. Proper designed airflow will lead to perfect cooling & improve efficiency [1-4].

Bypass air and recirculation are the most challenging issues when considering air flow management. Bypass air flow is cold supply air that is returning back to CRAC without passing through telecom racks. Recirculation is the bypass air partner. When insufficient air is delivered to the rack, the racks will compensate missed air by pulling it from warm air circulating nearby.

In this work, we are going to focus on hot air recirculation and cold air bypass around racks and predict the associated effect of non-uniformity and increase of air temperature entering racks. The conclusions of this study could be used as a reference to plan new open aisle data centers or to renovate existed data centers.

2. Research Methodology

2.1 Case Study

The dissertation will take Canar Telecommunication Company data center located at Khartoum, Sudan as a case study. This data center contains four down flow Computer Room Air – Conditioning (CRAC) units installed inside the servers’ room. The CRACs unit was part of the raised floor room layout with cooling air passing through plenum and venting in the room through vent tiles. The racks were arranged in three rows and have individual air flow and heat load. Heat dissipation and air flow rate were defined for all racks from the specifications model of the Icepack software. The description of data center and data center components, air flow through racks and vent tiles are summarized below;

Table 1: Data Center Description

Data Center layout	Raised Floor with Room Return
Room Dimensions	L=19m ,W=7.76m , H=3.05
Supply Plenum Height	0.5m
Number of CRAC Unit	4
Total flow Through CRAC Units	12 m ³ /s
Supply Air Temperature	17 °C
Number of Rack Rows	3
Total Number of Racks	44
Total Racks Heat load	144 KW
Heat load of Rack - 0 to Rack – 5 (located at Row -1)	3 KW
Heat load of Rack – 6 to Rack – 15 (located at Row -1)	7 KW
Number of Tile Rows	2
Number of Tile for Each Row	22
Tile Open Area	50%

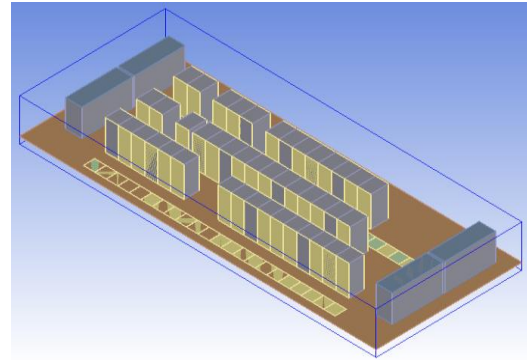


Figure 1: A 3D Model of Data Center

2.2 The Objective

The purpose of this study is to adopt accepted modifications for air flow parameters in order to minimize the effect of bypass air and recirculation inside data center so as to increase cooling efficiency and reduce power consumption.

3. Computational Fluid Dynamics (CFD)

3.1 Mathematical Model

The commercial CFD software package Icepack 18 was used as a basic tool for the simulation. Turbulent and zero equation for the flow regime has been used as recommended for such cases [5].

During the simulation the followings assumptions have been considered;

1. The flow as steady turbulent flow because the velocity of sound is greater than the indoor air velocity.
2. Adiabatic walls were chosen for the room. The room was isolated and the effects of heat transfer outside it were neglected.
3. The effects of radiation were ignored in the room according to the steady heat assumption, and heat transfer on the surface of the server was uniform.

4. The impact of disturbance from air leakage or personnel movement was ignored.

3.2 Continuity and Momentum Equations

The motion of each phase was governed by the corresponding mass and momentum conservation equations. The continuity equation is:

$$\frac{\partial \rho}{\partial t} + \frac{\partial(\rho u_x)}{\partial x} + \frac{\partial(\rho u_y)}{\partial y} + \frac{\partial(\rho u_z)}{\partial z} = 0 \quad (1)$$

Where u_i is the velocity of the i-th phase. The subscript i represents the x, y or z axis. The equation for the conservation of momentum is:

$$\rho \left(\frac{\partial u_x}{\partial t} + \frac{\partial u_x}{\partial x} u_x + \frac{\partial u_x}{\partial y} u_y + \frac{\partial u_x}{\partial z} u_z \right) = \left(\frac{\partial \sigma_x}{\partial x} + \frac{\partial \tau_{xy}}{\partial y} + \frac{\partial \tau_{xz}}{\partial z} \right) + f_x' \quad (2a)$$

$$\rho \left(\frac{\partial u_y}{\partial t} + \frac{\partial u_y}{\partial x} u_x + \frac{\partial u_y}{\partial y} u_y + \frac{\partial u_y}{\partial z} u_z \right) = \left(\frac{\partial \sigma_y}{\partial y} + \frac{\partial \tau_{yx}}{\partial x} + \frac{\partial \tau_{yz}}{\partial z} \right) + f_y' \quad (2b)$$

$$\rho \left(\frac{\partial u_z}{\partial t} + \frac{\partial u_z}{\partial x} u_x + \frac{\partial u_z}{\partial y} u_y + \frac{\partial u_z}{\partial z} u_z \right) = \left(\frac{\partial \sigma_z}{\partial z} + \frac{\partial \tau_{zx}}{\partial x} + \frac{\partial \tau_{zy}}{\partial y} \right) + f_z' \quad (2c)$$

$$\sigma_i = -p + 2\mu \frac{\partial u_i}{\partial i}, \quad \tau_{ij} = \mu \left(\frac{\partial u_i}{\partial j} + \frac{\partial u_j}{\partial i} \right) \quad (3)$$

where ρ is density in kg/m³; f_i is the interfacial force acting on phase i due to the presence of phase j, which includes drag force, interphase turbulent dispersion force, virtual mass and lift force [6,8]; μ is shear viscosity in N·s/m²; and p is pressure in N/m².

The energy equation is as follows:

$$\frac{\partial(\rho T)}{\partial t} + \frac{\partial(\rho u_x T)}{\partial x} + \frac{\partial(\rho u_y T)}{\partial y} + \frac{\partial(\rho u_z T)}{\partial z} = \frac{\partial}{\partial x} \left(\frac{k}{c_p} \frac{\partial T}{\partial x} \right) + \frac{\partial}{\partial y} \left(\frac{k}{c_p} \frac{\partial T}{\partial y} \right) + \frac{\partial}{\partial z} \left(\frac{k}{c_p} \frac{\partial T}{\partial z} \right) + S_T \quad (4)$$

Where T is the fluid temperature in K, c_p is the specific heat capacity of the fluid at constant pressure in J/gK, k is the fluid thermal transfer coefficient in m²/s and S_T is the term for viscous dissipation.

3.3. Turbulence Model

The zero – equation turbulence model has been used.

$$\mu_T = \rho l_{mix}^2 \left| \frac{dU}{dy} \right| \quad (5)$$

Where l_{mix} is the mixing length, U is the main stream velocity and y is the direction normal to the main flow.

3.4 Boundary Conditions

For the calculations of the CFD, a finite-volume approximation of the Reynolds-averaged Navier–Stokes equations and energy equations with the turbulent and zero equation model were solved. Ideal gas law is used as it is recommended for problems involving significant temperature difference.

Grid generation is very important for CFD calculations because it is directly related to its success or failure. The grid should meet the following criteria: the change in density in the grid domain should be based on the variables, and the change in elements in the entire solution domain should be smooth.

The quality of mesh was satisfactory because the calculated face alignment was greater than 0.7, which meant that no element had been severely distorted.

The boundary conditions, the initial conditions and the iteration scheme were set for the numerical simulations in the Icepack 18 software package. The pressure was discretized using the body force weighted scheme and the momentum and temperature through the first -order scheme.

The convergence criterion for flow was set at 1×10^{-7} and that for energy and H₂O specie was set at 1×10^{-3} . The simulation was stopped when it was determined to have reached a steady state. Used solution was confirmed independent from Mesh.

The relaxation factors are shown in the below table

Table 2: Factors concerning relaxation

Pressure	Momentum	Temperature	Viscosity	Body force	potential heating	Joule	H ₂ O
0.3	0.2	1	1	0.1	1	1	1

3.5 Calculation Method

In order to study the thermal and bypass phenomena, two assessment indexes will be used. Namely the β index and the energy utilization index η_r [9]. The β Index is proposed to evaluate the temperature rising in local rack [10] and this index could be defined as:

$$\beta = \frac{T_{in} - T_{ref}}{T_{out} - T_{in}} \quad (6)$$

Where T_{in} the mean temperature in the inlet, T_{out} is the mean temperature in the outlet, T_{ref} is the reference cooling temperature. The β index ranges are between 0 and 1. When the β index value is 0, it illustrates no recirculation of airflow. While the β index value is above 1, it means the phenomenon of self-heating.

In order to meet the utilization energy efficiency of airflow, energy utilization index is corrected and its expression is [11]:

$$\eta_r = \frac{T_{out} - T_{ref}}{\frac{T_{out} + T_{in}}{2} - T_{ref}} \quad (7)$$

Where T_{out} the air temperature in the outlet is, T_{in} is the air temperature in the inlet and T_{ref} is the air temperature of the cooling in the rack. In Equation (7), the low η_r shows a bad airflow organization, and has a hot air self-circulation between racks.

4. Results and Discussion

4.1 Open Aisle Data Center

Proper layout of racks is one of the parameters that may affect thermal management inside data centers. Normally racks are placed in a row in a contiguous manner. However, there may be gaps between them. These gaps are created by removing the racks or replacing them by another one smaller in size. Hot air from the back of the racks can leak inside the cold aisle through these gaps and increase the temperature of air entering into the racks. Fig 2 shows a plot of temperature distribution across a data center.

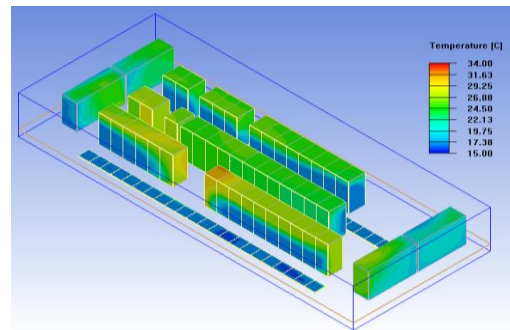


Figure 2: Temperature contours inside data Center

The highest temperature recorded inside the data center was at the rack closest to gap in row 1.

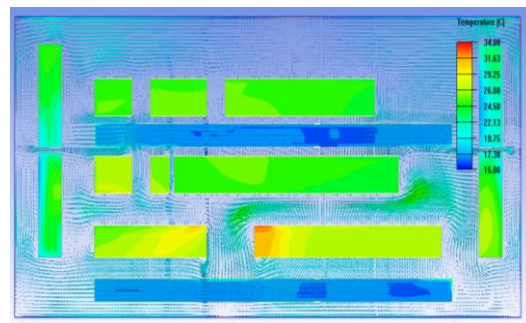


Figure 3: Temperature contours and velocity vectors on a horizontal plane

Fig 3 shows the velocity vector inside data center. Hot Air from the back of the racks leaked to the cold aisle and increased the inlet temperature of air entering racks. In order to minimize this recirculation, partitions are recommended to be installed to close the gaps between the racks.

4.2 Data Center with Partitions

In order to enhance the air flow distribution inside the data center, seven partitions will be installed to close the gaps between the racks to isolate the hot aisle from the cold aisle. The use of partitions is inexpensive and a fast solution. Fig. 4 shows the contours of temperature inside the data center after installing partitions.

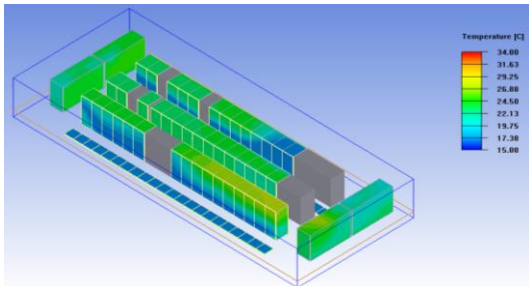


Figure 4: Use of partitions to prevent hot air recirculation

From Fig 5, the air flow becomes more uniform after closing the gaps between the racks and the global temperature was reduced.

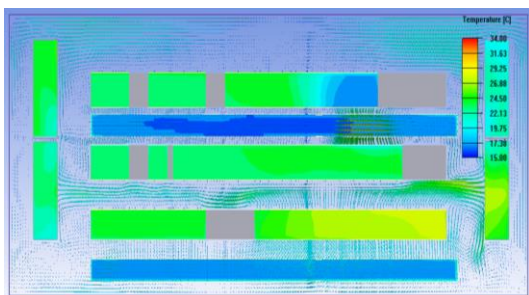


Figure 5: Temperature contours and velocity vectors on a horizontal plane of data center with partitions

4.3 Investigation of Data Center on Rack Level

Further investigation for air flow distribution inside the data center could be done based on rack level. One row contains racks with high heat density will be considered for analysis (highlighted in red at Fig 6).

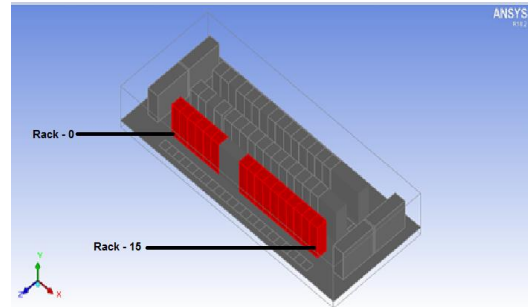


Figure 6: High density rack in data center

β index and the energy utilization index η_r , defined by equations 6 & 7 are used for this study. Results are shown on Figures 7 and 8 below. It is obvious that rack no. 6 has got the maximum value of β index and the minimum value of energy utilization index. This is due to the hot air recirculation from the hot aisle to the inlet of rack 6 through the nearest gap.

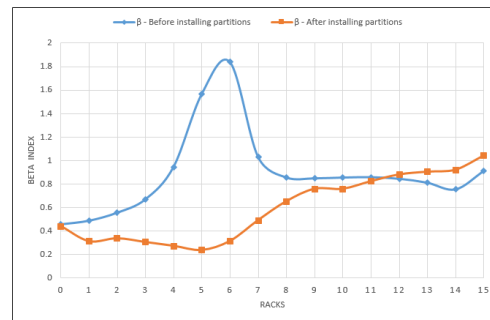


Figure 7: Beta Index before and after installing partitions

After closing all the gaps between the racks, the air flow distribution index was all enhanced. β index and energy utilization index η_r of Rack 6 improved.

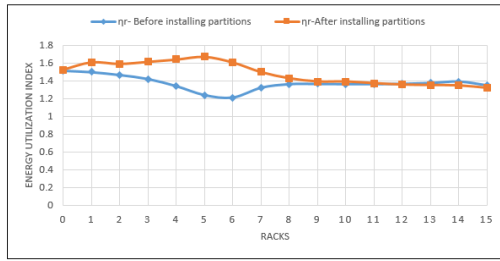


Figure 8: Energy utilization index before and after installing partitions

4.4 Effect of Airflow Outlet Angle

In standard tiles, air leaves at an outlet flow angle of 90°. This leads part of the cold air to bypass without passing through the racks. In order to reduce this effect, directional perforated tiles will be used to guide cold air towards the racks. Different air flow outlet angles from tiles will be investigated and the corresponding values of β index and energy utilization index will be evaluated to determine the best air flow outlet angle.

Table 3: β index for different air flow outlet angle

Rack	30°	45°	60°	75°	90°	120°
0	0.55	0.40	0.32	0.27	0.44	0.63
1	0.49	0.37	0.30	0.27	0.31	0.53
2	0.50	0.42	0.36	0.33	0.34	0.49
3	0.50	0.42	0.35	0.31	0.30	0.48
4	0.47	0.39	0.33	0.28	0.27	0.46
5	0.43	0.36	0.30	0.25	0.24	0.45
6	0.53	0.45	0.39	0.33	0.31	0.54
7	0.77	0.66	0.58	0.52	0.49	0.76
8	0.92	0.81	0.72	0.66	0.65	0.92
9	0.97	0.86	0.76	0.70	0.76	0.94
10	1.03	0.91	0.81	0.74	0.76	0.98
11	1.10	0.98	0.87	0.80	0.82	1.03
12	1.12	1.01	0.91	0.84	0.88	1.02
13	1.02	0.95	0.88	0.82	0.90	0.97
14	0.93	0.82	0.77	0.74	0.92	0.91
15	1.08	0.94	0.84	0.73	1.04	1.10

From table 3, the maximum values of β index are at angle 120°. This is because cold air from the tiles is mixed with the room warm air before entering the racks. At flow outlet angles of 30°, 45° & 60° the quantity of bypassed air is reduced and the temperature of air entering the racks becomes colder. At air flow outlet angle of 90°, the air index values became better than the previous angles. The minimum values of β index are at air flow outlet angle of 75°.

From table 4, with the increase of air flow outlet angle the energy utilization index increased. The peaks values are at air flow outlet angles of 75° & 90°. The minimum values of energy utilization efficiency are at air flow outlet angle of 120°.

Table 4: Energy utilization efficiency for different air flow outlet angle

Rack	30°	45°	60°	75°	90°	120°
0	1.47	1.55	1.61	1.65	1.53	1.44
1	1.51	1.57	1.62	1.65	1.62	1.49
2	1.50	1.55	1.58	1.60	1.60	1.50
3	1.50	1.55	1.59	1.62	1.62	1.51
4	1.52	1.56	1.61	1.64	1.65	1.52
5	1.54	1.58	1.62	1.67	1.68	1.53
6	1.48	1.52	1.56	1.60	1.61	1.48
7	1.39	1.43	1.46	1.49	1.50	1.40
8	1.35	1.38	1.41	1.43	1.43	1.35
9	1.34	1.37	1.40	1.42	1.40	1.35
10	1.33	1.35	1.38	1.40	1.40	1.34
11	1.31	1.34	1.36	1.39	1.38	1.33
12	1.31	1.33	1.35	1.37	1.36	1.33
13	1.33	1.35	1.36	1.38	1.36	1.34
14	1.35	1.38	1.39	1.40	1.35	1.35
15	1.32	1.35	1.37	1.41	1.32	1.31

Considering the values of beta Index & energy utilization index on table 3 and 4, the optimal outlet flow angle is 75°.

The airflow vectors of the CFD simulation at airflow angles of 30°, 45°, 60°, 75°, 90° & 120° are shown in Figure 9.

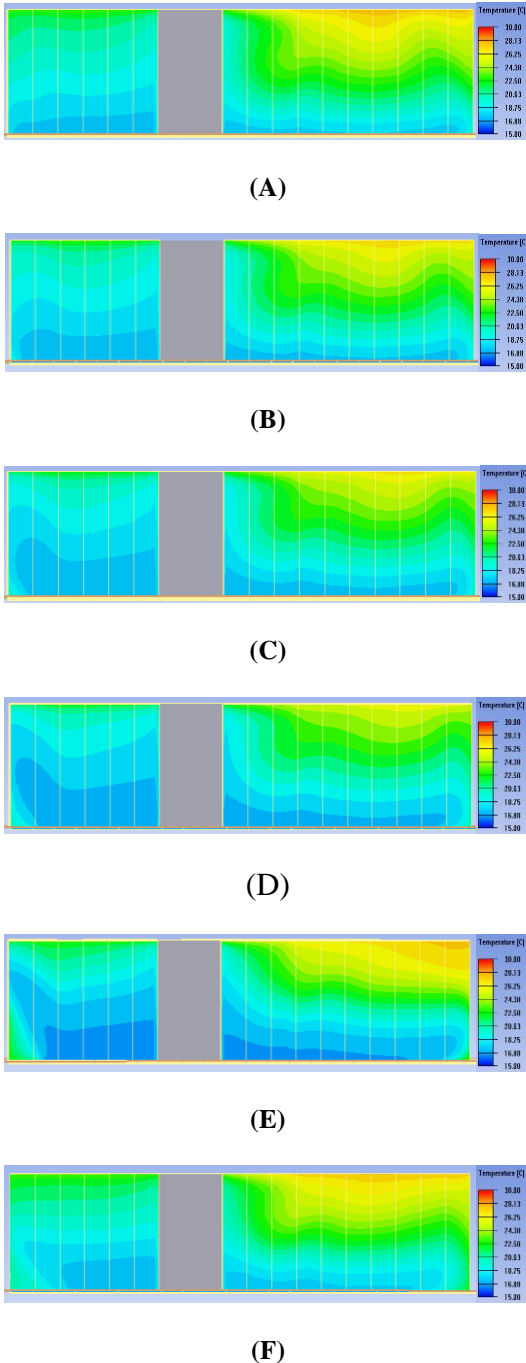


Figure 9: Temperature contour in the cold aisle: (A) 30°, (B) 45°, (C) 60°, (D) 75°, (E) 90° (F) 120°

Figure 9 shows the contours of local temperature of Row 1. The thermal distribution at an airflow outlet angle of 75° at the tiles was the optimal.

The temperature at the upper part of the racks is higher than the surrounding area due to circulation of air from hot aisle to cold aisle through the top side of the racks.

4.5 Effect of Supply Air Temperature

Supply of air temperature has an obvious influence on temperature distribution inside the data center. Using low supply air temperature will reduce the operating temperature of the conditioned equipment's and increase power required by air conditioning system and vice versa. In order to provide acceptable inlet temperature for racks, the temperature of cold air entering racks is normally reduced to overcome the effect of hot exhaust air recirculation. This often increases the energy cost of the data center. The optimal supply air temperature will ensure acceptable operating temperature for equipment's and low power consumption for air conditioning system. This will be achieved by studying beta and energy utilization indexes for each rack.

Table 5: β index for different supply air Temperature

Rack	15°C	16°C	17°C	18°C	19°C	20°C
0	0.30	0.30	0.27	0.30	0.30	0.30
1	0.28	0.28	0.27	0.28	0.28	0.28
2	0.33	0.34	0.33	0.34	0.34	0.34
3	0.31	0.32	0.31	0.32	0.32	0.32
4	0.29	0.29	0.28	0.29	0.29	0.29
5	0.27	0.27	0.25	0.28	0.28	0.28
6	0.35	0.34	0.34	0.35	0.35	0.35
7	0.52	0.52	0.52	0.53	0.53	0.53
8	0.66	0.66	0.66	0.66	0.67	0.67
9	0.70	0.71	0.70	0.71	0.71	0.71
10	0.74	0.74	0.74	0.75	0.75	0.75
11	0.80	0.80	0.80	0.80	0.81	0.81
12	0.83	0.56	0.84	0.84	0.85	0.85
13	0.82	0.82	0.82	0.83	0.83	0.83
14	0.74	0.74	0.74	0.75	0.75	0.75
15	0.78	0.79	0.73	0.79	0.79	0.80

From table 5, the values of beta for all supply air temperature are almost in a stable region.

Table 6: Energy efficiency index for different supply air Temperature

Rack	15°C	16°C	17°C	18°C	19°C	20°C
0	1.63	1.63	1.65	1.63	1.63	1.62
1	1.64	1.64	1.65	1.64	1.64	1.64
2	1.60	1.60	1.60	1.60	1.60	1.60
3	1.61	1.61	1.62	1.61	1.61	1.61
4	1.63	1.63	1.64	1.63	1.63	1.63
5	1.65	1.65	1.67	1.64	1.64	1.64
6	1.59	1.59	1.60	1.59	1.59	1.59
7	1.49	1.49	1.49	1.49	1.49	1.49
8	1.43	1.43	1.43	1.43	1.43	1.43
9	1.42	1.41	1.42	1.41	1.41	1.41
10	1.40	1.40	1.40	1.40	1.40	1.40
11	1.39	1.39	1.39	1.38	1.38	1.38
12	1.38	1.47	1.37	1.37	1.37	1.37
13	1.38	1.38	1.38	1.38	1.38	1.37
14	1.40	1.40	1.40	1.40	1.40	1.40
15	1.39	1.39	1.41	1.39	1.39	1.39

From table 6, the maximum values of energy efficiency index are at air supply temperature of 17°C. Therefore, based on table 5 & 6, the optimal supply air temperature is 17°C.

Fig 10 shows the temperature contours inside the data center with air flow outlet angle of 75° for tiles supplied air to racks located at row 1 with supply air temperature of 17°C.

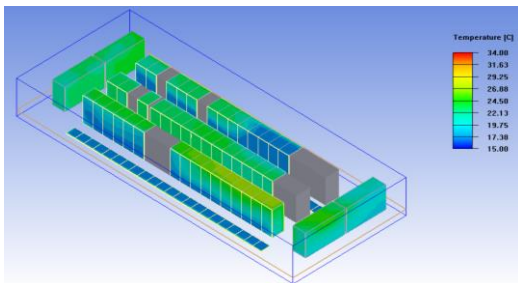


Figure 10: Temperature Contours inside data Center

4.6 Effect of Tile Open Area

Air flow rate from perforated tiles has direct effect on heat transfer inside servers. Increasing the tile open area will increase the flow rate and vice versa. Using of suitable tile open area will

optimize air flow distribution. Optimal tile open area will be investigated by using β index and utilization energy efficiency.

Table 7: β index for different tile open area

Rack	50%	60%	70%	80%
0	0.27	0.17	0.16	0.15
1	0.27	0.15	0.14	0.13
2	0.33	0.15	0.14	0.13
3	0.31	0.15	0.14	0.13
4	0.28	0.14	0.13	0.12
5	0.25	0.12	0.11	0.10
6	0.34	0.18	0.17	0.16
7	0.52	0.29	0.26	0.24
8	0.66	0.37	0.35	0.32
9	0.70	0.43	0.41	0.38
10	0.74	0.44	0.39	0.35
11	0.80	0.44	0.26	0.35
12	0.84	0.46	0.41	0.36
13	0.82	0.47	0.44	0.38
14	0.74	0.46	0.45	0.39
15	0.73	0.53	0.54	0.48

With the increase of the tile open area, β index decreased. Major decrease occurred at tile open area of 60%. Further increase of tile open area of more than 60% will decrease the values of β index but with minor decrease on the values of β index.

Table 8: Utilization energy index for different tile open area

Rack	50 %	60 %	70 %	80 %
0	1.65	1.74	1.76	1.77
1	1.65	1.77	1.78	1.80
2	1.60	1.76	1.78	1.79
3	1.62	1.77	1.78	1.79
4	1.64	1.78	1.80	1.81
5	1.67	1.80	1.82	1.83
6	1.60	1.73	1.74	1.76
7	1.49	1.64	1.66	1.67
8	1.43	1.57	1.59	1.61
9	1.42	1.54	1.55	1.57
10	1.40	1.53	1.56	1.59
11	1.39	1.53	1.66	1.59
12	1.37	1.52	1.55	1.58

13	1.38	1.51	1.53	1.57
14	1.40	1.52	1.53	1.56
15	1.41	1.49	1.48	1.51

With the increase of tile open area, utilization energy efficiency increased. The major increment occurred at tile open area of 60%. Further increase of tile open area will increase the values of utilization energy index. From table 7 & 8, the optimal percentage of open area for tiles supply air to row 1 is 60%. To have better insight of the effect of tile open area on temperature distribution inside the data center, plane cut through y-axis will be investigated.

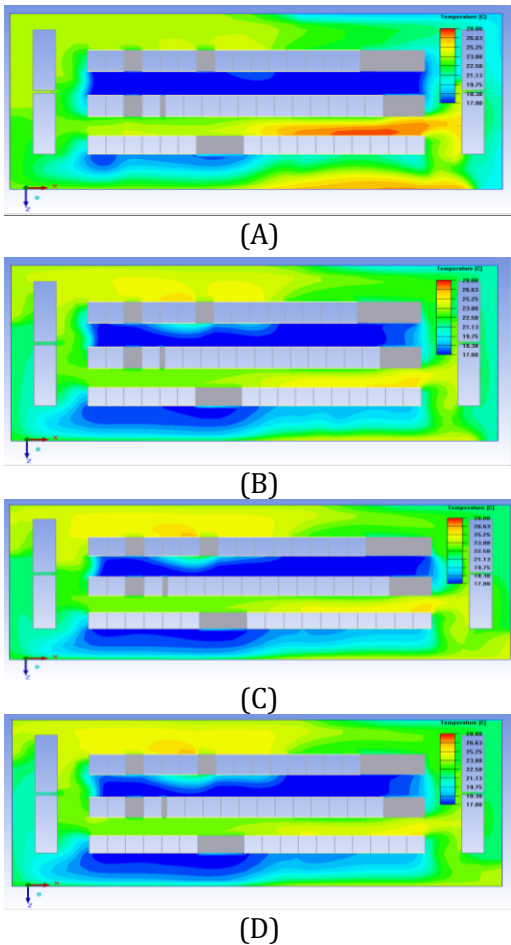


Figure 11: Temperature contour at XZ plane (Y=1.525m) inside data center for different tile open area of row 1: (A) 50%, (B) 60%, (C) 70%, (D) 80%

The optimal flow rate is achieved when hot airflow concentrates in the hot aisle with less mixing of air at the cold aisle. Also the majority of cold air should pass through the racks to hot aisle with less bypass air.

From Figure 11, hot air recirculation exists through row 1 when using tile open area of 50%. This effect is reduced by increasing of tile open area from 50% to 60%. Further enlargement of open area more than 60% will have minor effect and consume more cold air.

Fig 12 shows the temperature contours inside the data center at supply temperature of 17°C and tile supplied air to Row1 with open area of 60% and air outflow angle of 75°.

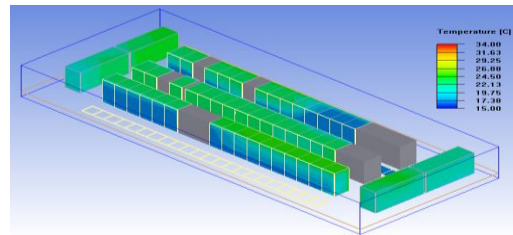


Figure 12: Temperature contours inside data center

The thermal distribution of row 1 is enhanced as shown in Figure 13. However, the performance of racks located at the end of row is poor due to bypass and recirculation from end sides.

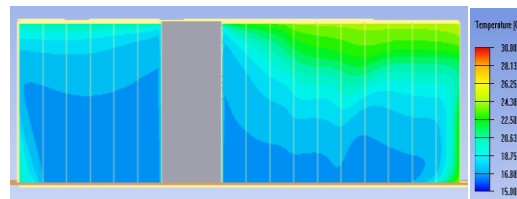


Figure 13: Temperature contour in the cold aisle of row 1 at 17°C, tile of air flow outlet angle 75° and tile open area of 60%

4.7 End Effect

Racks located in the middle of the data center have better air flow distribution than racks located closed to the computer room air conditioner units. The reason behind this, is the

pressure distribution under the raised floor. For this reason, racks with high heat density is recommended to be installed far away from computer room air conditioner unit so as to ensure enough air flow rate.

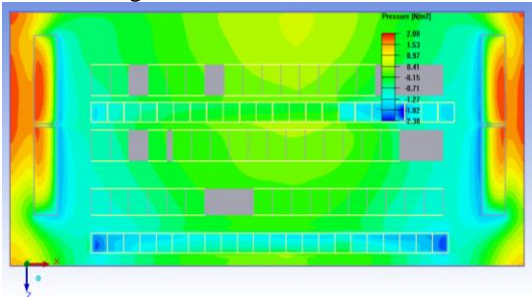


Figure 14: Pressure distribution under raised floor at XZ plane (y= 0.445 m)

Considering the current data center under study, the high density racks which are located at the end of row 1 require a lot of air flow since they suffer from insufficient air flow. For this reason, air is returned from the hot aisle to the inlet of racks and thus increase the temperature of air supply.

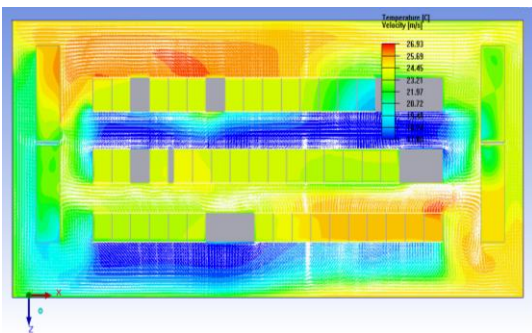


Figure 15: Temperature contours and velocity vector at XZ plane (Y=1.525m)

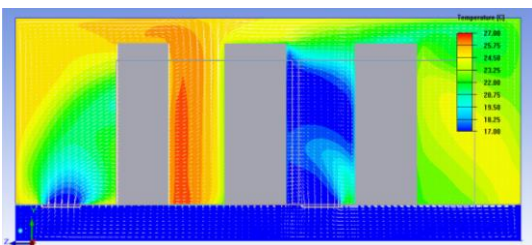


Figure 16: Temperature contours and velocity vector at YZ plane (x=15.96m)

In order to enhance the air distribution at the end of the row we need to prevent hot air returning to the inlet of the racks. The suggested remedy is to install additional tiles at the both ends of Row-1 to act like an air curtain as shown in Fig 17.

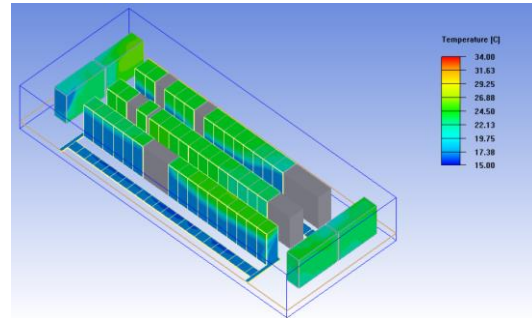


Figure 17: Temperature contours inside data center for supply air temperature of 17°, air flow outlet angle of 75° for Row 1 and air curtain

After installing air curtains at both ends of tiles supply air to row 1, the temperature contour in the cold aisle is improved as shown in Figure 18 and Figure 19 below.

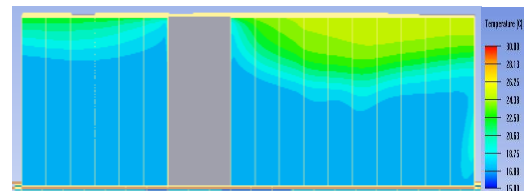


Figure 18: Temperature contour in the cold aisle of row 1 at 17°C, tile of air flow outlet angle 75° and tile open area of 60% with air curtain

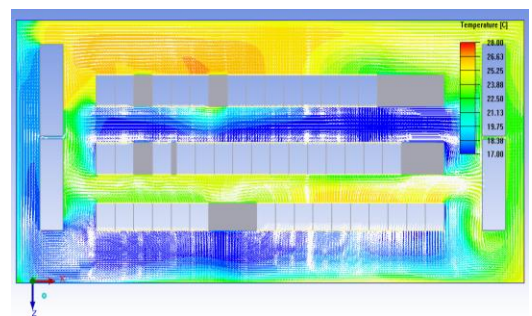


Figure 19: Temperature contours and velocity vector at XZ plane (Y=1.525m)

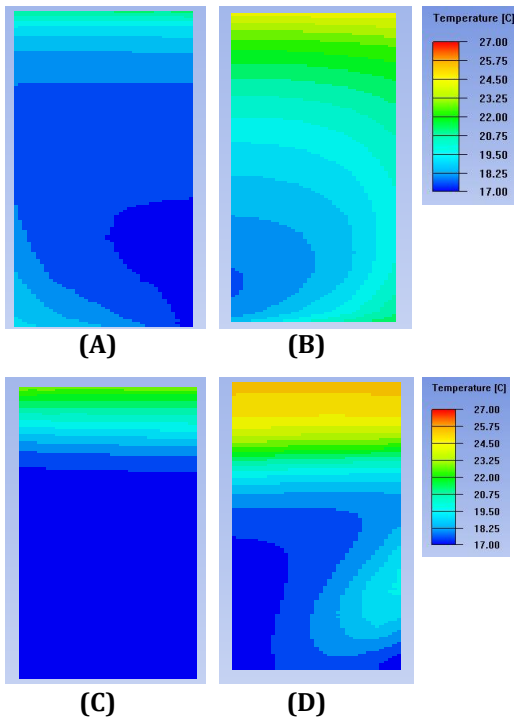


Figure 20: Temperature contour in the cold aisle (A) rack 0 before installing air curtain, (B) rack 15 before installing air curtain, (C) rack 0 after installing air curtain, (D) rack 15 after installing air curtain

The temperature distribution of the end racks was improved after installing air curtains. This is because air recirculation is reduced from the end side by installing air curtain. However, there is still recirculation from the top side of the racks causing the upper side of the racks to become non-uniform. For this reason closed aisle data center is recommended wherever possible.

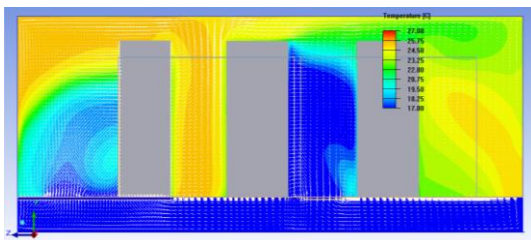


Figure 21: Temperature contours and velocity vector at YZ plane (x=15.96m) after installing air curtain

5. Conclusions

Data center has been simulated using CFD simulation software (Icepack). Temperature distribution across data center was showed and the effect of gaps between the racks was highlighted. Data center was rectified by closing gaps with partitions in order to prevent hot air recirculation from hot aisle to cold aisle. Results showed improved temperature distribution after this remedy. The effect of air flow outlet angle was analyzed using beta index and energy utilization index. Different air flow outlet angles were tested. The minimum beta index and a maximum energy utilization index were at an angle of 75°C, which represented better air distribution. Using the same approach for the supply air temperature, the optimal value was found at 17°C. Also the effect of tile Open area was investigated considering optimal parameters obtained for outlet flow angle & air supply temperature. The best tile open area founded for this case was 60%. End effect of racks was showed and reduced by using additional tiles to act like an air curtain. This study indicates the importance of CFD simulation to analyze air flow inside the data center and choosing the optimal operating parameters.

Acknowledgments

The authors extend their thanks and appreciation for the support of Canar Telecommunication Company and the School of Mechanical Engineering, Sudan University of Science & Technology (SUST).

References

- [1] Wang, I.N.; Tsui and Y.Y.; Wang C.C. Improvements of Airflow Distribution in a Container Data Center. *Energy, Proc.* 2015, 75, 1819–1824.
- [2] Cho, J.; Lim, T.; Kim, B.S. Measurements and predictions of the air distribution systems in high compute density (internet) data centers. *Energy Build.* 2009, 41, 1107–1115.
- [3] Lu, T.; Lü, X.; Remes, M. Investigation of air management and energy performance in

- a data center in Finland: Case study. *Energy Build.* 2011, 43, 3360–3372.
- [4] Hosseini, S.H.; Shokry, E.; Ahmadian Hosseini, A.J.; Ahmadi, G.; Calautit, J.K. Evaluation of airflow and thermal comfort in buildings ventilated with wind catchers: Simulation of conditions in Yazd City, Iran.
- [5] *Energy Sustain. Dev.* 2016, 35, 7–24. A zero-equation turbulence model for indoor airflow simulation (<https://www.sciencedirect.com/science/article/abs/pii/S0378778898000206>).
- [6] Ansys Incorporated. ANSYS FLUENT-Solver Release 10.0; Ansys Inc.: Canonsbury, PA, USA 2005; p. 131.
- [7] Abanto, J.; Barrero, D.; Reggio, M.; Ozell, B. Airflow modeling in a computer room. *Build. Environ.* 2004, 39, 1393–1402.
- [8] Song, Z. Thermal performance of a contained data center with fan-assisted perforations. *Appl. Therm. Eng.* 2016, 102, 1175–1184.
- [9] Ni, J.; Jin, B.; Zhang, B.; Wang, X. Simulation of airflow distribution and analysis of energy consumption in data centers with a confined space. *Sustainability* 2017, 9, 664.
- [10] Arghode, V.K.; Kumar, P.; Joshi, Y.; Weiss, T.; Meyer, G. Rack Level Modeling of Air Flow Through Perforated Tile in a Data Center. *J. Electron. Packag.* 2013, 135, 030902.
- [11] Xu, Q. Energy Consumption and Air Distribution Simulation of a Substation Data Room. Master's Thesis, Zhejiang University, Hangzhou, China, 2015.